View metadata, citation and similar papers at core.ac.uk

brought to you by CORE

provided by Digital Repository @ Iowa State University

IOWA STATE UNIVERSITY
Digital Repository

Civil, Construction and Environmental Engineering Publications

Civil, Construction and Environmental Engineering

2-2013

Pile Setup in Cohesive Soil. I: Experimental Investigation

Kam W. Ng
University of Wyoming

Flad Architects

Sherif S. AbdelSalam
British University in Egypt

See next page for additional authors

Follow this and additional works at: https://lib.dr.iastate.edu/ccee_pubs


Part of the Civil Engineering Commons, Construction Engineering and Management Commons, and the Geotechnical Engineering Commons

The complete bibliographic information for this item can be found at https://lib.dr.iastate.edu/ccee_pubs/162. For information on how to cite this item, please visit http://lib.dr.iastate.edu/howtocite.html.

This Article is brought to you for free and open access by the Civil, Construction and Environmental Engineering at Iowa State University Digital Repository. It has been accepted for inclusion in Civil, Construction and Environmental Engineering Publications by an authorized administrator of Iowa State University Digital Repository. For more information, please contact digirep@iastate.edu.

Pile Setup in Cohesive Soil. I: Experimental Investigation

Abstract
Pile setup in cohesive soils has been a known phenomenon for several decades. However, a systematic field investigation to provide the needed data to develop analytical procedures and integrate pile setup into the design method rarely exists. This paper summarizes a recently completed field investigation on five fully instrumented steel H-piles embedded in cohesive soils, while a companion paper discusses the development of the pile setup method. During the field investigation, detailed soil characterization, monitoring of soil total lateral stress and pore-water pressure, collection of pile dynamic restrike data as a function of time, and vertical static load tests were completed. Restrike measurements confirm that pile setup occurs at a logarithmic rate following the end of driving, and its development correlates well with the rate of dissipation of the measured porewater pressure. Based on the field data collected, it was concluded that the skin friction component, not the end bearing, contributes predominantly to the setup, which can be accurately estimated for practical purposes using soil properties, such as coefficient of consolidation, undrained shear strength, and the standard penetration testN-value.

Keywords
Pile setup, Load tests, Cohesive soil, Coefficient of consolidation, Undrained shear strength, Standard penetration test (SPT) N-value

Disciplines
Civil Engineering | Construction Engineering and Management | Geotechnical Engineering

Comments
This is a manuscript of an article published as Ng, Kam W., Matthew Roling, Sherif S. AbdelSalam, Muhannad T. Suleiman, and Sri Sritharan. "Pile setup in cohesive soil. I: experimental investigation." Journal of Geotechnical and Geoenvironmental Engineering 139, no. 2 (2012): 199-209. doi: 10.1061/(ASCE)GT.1943-5606.0000751. Posted with permission.

Authors
Kam W. Ng, Flad Architects, Sherif S. AbdelSalam, Muhannad T. Suleiman, and Sri Sritharan

This article is available at Iowa State University Digital Repository: https://lib.dr.iastate.edu/ccee_pubs/162

ResearchGate

See discussions, stats, and author profiles for this publication at: https://www.researchgate.net/publication/273432439

Pile Setup in Cohesive Soil. I: Experimental Investigation

Article *in* Journal of Geotechnical and Geoenvironmental Engineering · February 2013

DOI: 10.1061/(ASCE)GT.1943-5606.0000751

CITATIONS
28

READS
159

5 authors, including:

Kam Ng
University of Wyoming
40 PUBLICATIONS **100** CITATIONS
SEE PROFILE

Sherif S. Abdelsalam
Nile University
26 PUBLICATIONS **106** CITATIONS
SEE PROFILE

Muhannad T. Suleiman
Lehigh University
87 PUBLICATIONS **647** CITATIONS
SEE PROFILE

Sri Sritharan
Iowa State University
193 PUBLICATIONS **1,383** CITATIONS
SEE PROFILE

Some of the authors of this publication are also working on these related projects:

Deep Foundation View project

Pavement Design View project

All content following this page was uploaded by Kam Ng on 08 April 2015.

The user has requested enhancement of the downloaded file.

Journal of Geotechnical and Geoenvironmental Engineering, 139(2), February 2013, pp. 199-209

PILE SETUP IN COHESIVE SOIL. I: An Experimental Investigation

By

Kam W. Ng, Ph.D.
Assistant Professor
University of Wyoming, Email: kng1@uwyoedu

Matthew Roling
Structural Engineer
Flad Architects, Email: matthew.roling@gmail.com

Sherif S. AbdelSalam, Ph.D.
Lecturer
British University in Egypt, E-mail: sherif.abdelsalam@bue.edu.eg

Muhannad T. Suleiman, Ph.D.
P.C. Rossin Assistant Professor
Lehigh University, Email: mts210@lehigh.edu

Sri Sritharan, Ph.D.
(Corresponding Author)
Wilson Engineering Professor
Iowa State University, Email: sri@iastate.edu

Manuscript Accepted Not Copyedited

Words: 5340

Figure and Tables: 4572

Total Word Count: 9912

Manuscript Accepted as Technical Paper To:

ASCE Journal of Geotechnical and Geoenvironmental Engineering

Journal of Geotechnical and Geoenvironmental Engineering, 139(2), February 2013, pp. 199-209

PILE SETUP IN COHESIVE SOIL. I: An Experimental Investigation

Ng, K. W.[1]; Roling, M.[2]; AbdelSalam, S. S.[3]; Suleiman, M. T.[4]; and Sritharan, S.[5]

ABSTRACT: Pile setup in cohesive soils has been a known phenomenon for several decades. However, a systematic field investigation to provide the needed data to develop analytical procedures and integrate pile setup into the design method rarely exists. This paper summarizes a recently completed field investigation on five fully instrumented steel H-piles embedded in cohesive soils, while a companion paper discusses the development of the pile setup method. During the field investigation detailed soil characterization, monitoring of soil total lateral stress and pore water pressure, collection of pile dynamic restrike data as a function of time, and vertical static load tests were completed. Restrike measurements confirm that pile setup occurs at a logarithmic rate following the end of driving, and its development correlates well with the rate of dissipation of the measured pore water pressure. Based on the field data collected it was concluded that the skin friction component, not the end bearing, contributes predominantly to the setup, which can be accurately estimated for practical purposes using soil properties, such as coefficient of consolidation, undrained shear strength and/or SPT *N*-value.

CE Database Keywords: Pile setup; Load tests; Cohesive soil; Coefficient of consolidation; SPT *N*-value.

Manuscript Accepted Not Copyedited

[1] Assistant Professor, Dept. of Civil and Architectural Engineering, University of Wyoming, Laramie, WY 82071. E-mail: kng1@uwyo.edu
[2] Structural Engineer, Flad Architects, E-mail: matthew.roling@gmail.com
[3] Lecturer, British University in Egypt, E-mail: sherif.abdelsalam@bue.edu.eg
[4] P.C. Rossin Assistant Professor, Dept. of Civil and Environmental Engineering, Lehigh University, Bethlehem, PA, 18015. E-mail: mts210@lehigh.edu
[5] Wilson Engineering Professor and Associate Chair, Dept. of Civil, Construction and Environmental Engineering, Iowa State University, Ames, IA 50011. E-mail: sri@iastate.edu (Corresponding Author)

Journal of Geotechnical and Geoenvironmental Engineering, 139(2), February 2013, pp. 199-209

INTRODUCTION

Many researchers and practitioners have recognized the increase in resistance (or capacity) of driven piles embedded in cohesive soils over time; a phenomenon referred to as pile setup. Pile setup occurs due to the healing of remolded cohesive soils, an increase in lateral stresses, and dissipation of pore water pressure (Soderberg 1962, and Randolph et al., 1979). When accounted for accurately, the integration of pile setup in the pile design process can lead to a more cost-effective design as it reduces the number of piles and/or the length of piles. Unfortunately, experimental data combined with a dependable method to account for pile setup is rarely available.

Static or dynamic tests can be performed to evaluate pile setup; however, it is not feasible in practice to perform these tests over a period of time, as acknowledged by the American Association of State Highway and Transportation Officials (AASHTO) (2010). Empirical methods to estimate pile setup have been proposed by several researchers, such as Pei and Wang (1986), Skov and Denver (1988) and Svinkin and Skov (2000). However, these methods have several shortcomings. For instance, Pei and Wang's (1986) method was purely empirical, specifically developed for Shanghai soil, and lacked generalization in terms of soil properties. Skov and Denver's (1988) and Svinkin and Skov's (2000) methods require site specific calibration of pile setup factors with restrike data since the factors are not correlated with soil properties. Due to insufficient experimental data, these methods have not been substantially validated for accurate practical applications. For these reasons, empirical methods to account for pile setup have not been included as part of the AASHTO (2010) LRFD Specifications.

To account for pile setup, the following information is needed for commonly used foundation types: a) sufficient and detailed dynamic and static field test data as a function of time for accurate setup evaluation; and b) detailed subsurface investigations and monitoring of soil stresses to develop methods to quantify setup (Komurka et al., 2003). A literature review by the writers concluded that published information on pile setup lacks detailed dynamic and static field test data as a function of time for both small-displacement piles (i.e., H-piles and open-ended pipe piles) and large-displacement piles (closed-end pipe piles and precast concrete piles). In particular, quality setup data on small-displacement piles is relatively scarce according to the published data of pile setup reported by Long et al. (1999) and Komurka et al. (2003).

Manuscript Accepted Not Copyedited

Furthermore, despite the fact that pile setup is influenced by properties of the soil surrounding the pile and pore water pressure, the necessary data to quantitatively describe the relationship between pile setup, surrounding soil properties, and dissipation of pore water pressure is not available. If the influence of surrounding soils on pile setup is significant, then the dependency of pile setup on surrounding soil properties and pore water pressure needs to be studied. Given that a recent survey of more than 30 State Departments of Transportation (DOTs) conducted by AbdelSalam et al. (2010) revealed that steel H-pile is the most common foundation type used for bridges in the United States, the setup investigation reported herein focuses on this pile type.

BACKGROUND

Soil setup observations for various steel H-piles embedded in cohesive soils (see Figure 1) have been reported by Huang (1988) and Lukas & Bushell (1989), and more recently by Long et al. (2002) and Fellenius (2002). Figure 1 summarizes the pile setup reported in the literature for steel H-piles, in terms of a resistance ratio defined as the total pile resistance at any time after EOD (R_t) divided by the reference total pile resistance at EOD (R_{EOD}). The total pile resistances (R_t) were determined either from a static load test or based on Pile Driving Analyzer (PDA) measurements in conjunction with CAPWAP analysis at different times of restrike. The reference pile resistances at EOD (R_{EOD}) were based on CAPWAP analysis. For comparative purposes, a predominant soil type along the pile shaft and a weighted average SPT *N*-value (N_a) were determined for each data source. Figure 1 shows that pile resistances increase immediately after EOD, with the rate of increase decreasing over time. The extent of setup, however, varies between sites. Generally, it can be observed that piles embedded in a soil profile with a relatively small N_a value exhibited a higher resistance ratio (R_t/R_{EOD}), indicating a higher pile setup. However, the test pile reported by Lukas & Bushell (1989) exhibited a higher resistance ratio than that of Fellenius (2002) despite similar N_a values for both sites, confirming that setup is also influenced by other soil parameters. Although the mechanisms of pile setup are related to the increase in lateral stresses and dissipation of pore water pressure, there were no consolidation test results, in-situ lateral stresses, or pore water pressure measurements reported by the authors. Recognizing the difficulty in understanding pile setup based solely on the data available in the literature, the current study focused on collecting sufficient quality soil data for performing pile setup evaluations, including Standard Penetration Test (SPT) *N*-values, Piezocone Penetration

Manuscript Accepted Not Copyedited

Test (CPT) data, horizontal coefficient of consolidation (C_h), and Atterberg limits.

FIELD INVESTIGATION

Test Locations

As part of an effort to establish LRFD guidelines in Iowa, ten steel H- piles were driven and load tested in the field in different Iowa counties representing five geological regions (Ng et al., 2011a). Five of these piles were driven into cohesive soils to investigate the effects of setup. The test piles embedded in cohesive soil profiles are referred to as ISU2, ISU3, ISU4, ISU5, and ISU6 (see Figure 2). Test piles ISU2 at Mills County, ISU3 at Polk County, and ISU6 at Buchanan County were located in loess, Wisconsin glacial, and loamy glacial geological formations, respectively. Both ISU4 at Jasper County and ISU5 at Clarke County were in a geological formation of glacial clay topped with loess soil deposits. Following a detailed evaluation of results for ISU5 and ISU6, data from all five tests is used to develop a rational approach for quantifying pile setup. Refer to Ng et al. (2011a) for more detailed information.

Soil Characterizations

Each test site was characterized using in-situ subsurface investigations, which consisted of SPT tests and CPT with pore water pressure dissipation measurements, as well as laboratory soil classification and one-dimensional consolidation tests. SPTs and CPTs were performed within a distance of 3.7 m from test piles ISU2, ISU3, ISU5 and ISU6 and 15 m from test pile ISU4, which all have a consistent soil profile. Figure 3 summarizes the measured SPT N-values, the measured CPT tip resistance (q_c), and skin friction (f_s) along the piles ISU5 and ISU6. During the CPTs, pore water pressure dissipation tests were conducted at all sites. Based on the CPTs that achieved 50% pore water pressure dissipation, the values of C_h were estimated (see Table 1) using the strain path method by Houlsby and Teh (1988), which consists of a rigidity index (I_R) defined as the ratio of shear modulus (G) to undrained shear strength (S_u). In contrast, considering cavity expansion theory and critical-state soil mechanics, the I_R value can be evaluated directly from the CPT data (Mayne, 2001).

Disturbed soil samples were collected for laboratory soil classification in accordance with the Unified Soil Classification System (USCS). Table 1 includes the USCS analysis for all soil layers, including soil unit weight (γ), liquid limit (LL), and plasticity index (PI), which shows that almost all soil layers were classified as low plasticity clay (CL). In addition, undisturbed

Manuscript Accepted Not Copyedited

soil samples, collected using 75 mm Shelby tubes, were tested using one-dimensional consolidation tests in accordance with American Standard Testing Method (ASTM) D2435 (ASTM, 2004). Table 1 shows that the vertical coefficient of consolidation (C_v) values ranged from 0.033 to 0.152cm^2/min, and almost all soil layers at various sites were normally consolidated to slightly over-consolidated. The high over-consolidation ratio (*OCR*) values, above 4.0, obtained near the ground surface of ISU3 and ISU5 are suspected to be due to mechanical compaction of the top soil layers during past road construction; ISU3 was situated near the loop ramp of a cloverleaf interchange whereas ISU5 was located at an old road median.

For ISU5, the 7.6 m thick top low plasticity clay (CL) layer with loess origin underlays a glacial till layer classified as low plasticity clay with sand (CL). The ground water table (GWT) was located approximately 11 m below the ground surface. The 7.6 m thick low plasticity top clay layer was found to have an average SPT *N*-value of 8 overlaying sandy low plasticity clay with an average SPT *N*-value of 16. The C_v values ranged from 0.051 to 0.107 cm^2/min. For ISU6, which was situated in an outwash loamy glacial region, the soil profile was divided into four layers, consisting of 4 m of a mixed fill of clayey sand and low plasticity clay (SC and CL) overlaying 2.1 m of silty sand (SM), 9.05 m of sandy low plasticity clay (CL) with a 0.35 m silty sand seam (SM), and approximately 3.55 m of low plasticity silt (ML). The GWT was located approximately 4.6 m below the ground surface. The SPT *N*-values ranged from 8 to 23 with the softest layer of sandy low plasticity clay at a depth of 6.1 to 8.95 m. The C_h value at the 15.2 m depth was 0.008 cm^2/min., and the C_v values ranged from 0.033 to 0.057 cm^2/min.

Since the CPT dissipation test was not conducted for all soil layers at each site, because it requires an excessively long waiting time to achieve 50% pore water pressure dissipation during a CPT for a C_h estimation, the relationship between C_h and S_u was established in Figure 4(a) based on the tests where this data was acquired. Many researchers, such as Long et al. (1999), reported that driven piles embedded in soft clays experience more setup than in stiff clays, as observed in Figure 1 based on SPT *N*-value. Since the q_c value defined based on S_u has a relationship with SPT *N*-value plus the soil types were mostly CL soils with a relative small variation in mean grain size (Robertson et al., 1983), a compatible relationship between C_h and the most commonly used SPT *N*-value was established in Figure 4(b). For estimating conservative pile setup resistance, Mayne's (2001) approach of estimating the I_R value, that

Manuscript Accepted Not Copyedited

yields a smaller C_h, is recommended. Using this relationship, the C_h values were estimated for cohesive layers where the dissipation test was not performed. Due to limited measured soil data, this relationship should be used with engineering judgment, especially for S_u smaller than 50 kPa and SPT N-value smaller than 5. Table 2 lists the weighted average SPT N, S_u and C_h values along each pile shaft. These weighted average values were calculated by weighting the measured soil property for the cohesive soil layer by a layer-thickness-to-total-pile-length ratio for all cohesive layers located along the embedded pile length.

Instrumentation

All HP 250×62 test piles were instrumented with weldable vibrating strain gauges in pairs on either side of the web along the centerline of the embedded pile length as shown in Figure 3, with the lowest gauges installed within 150 mm of the toe. All strain gauges were covered with a black flexible rubber membrane and aluminum tape to protect them from welding sparks, heat, and moisture. The strain gauge cables were also wrapped with aluminum foil. The gauges and cables were covered with 50 mm × 50 mm × 5 mm steel angles welded to the webs of the pile to prevent damage caused by direct soil contact during pile installation. Despite the addition of the two steel angles, the shaft surface area in contact with the soil increased by only 4%. The steel angles were chamfered at the pile toe to form a pointed end, minimizing any increase in the toe cross-sectional area. Prior to the pile installation, two strain transducers and two accelerometers for PDA monitoring were installed 750 mm below the top of all test piles. The strain transducers were bolted to both sides of the web along the centerline, and the accelerometers were attached to either side of the web at a distance of 75 mm left and right of the strain transducers. The PDA recorded the strains and accelerations during pile driving and restrikes.

Push-In Pressure Cells

To measure the total lateral earth and pore water pressures during pile driving, restrikes and static load tests (SLTs), Geokon Model 4830 push-in pressure cells (PCs), fully saturated using a geotechnical hand pump, were inserted in the soil at a horizontal distance, ranging from 200 mm to 610 mm, from test piles ISU5 and ISU6; PCs were not installed near ISU2, ISU3 and ISU4. The PCs were installed one to two days prior to pile driving to allow stabilization of lateral stress and pore water pressure readings before testing. To install each PC, a 100 mm diameter borehole was drilled to a specified depth below the ground surface using a hollow-stemmed auger. The

Manuscript Accepted Not Copyedited

PC was then lowered through the hollow-stemmed auger and pushed approximately 350 mm below the bottom of the borehole, oriented such that the piezometer and the flat pressure surface faced the flange of the test pile. Measurements were taken every 4 sec during driving, restrikes and SLT, while readings were taken at 30 minute intervals between restrikes, as well as between the last restrike and SLT. The push-in pressure cell, denoted as PC1 in Figure 3(a), was installed approximately 7 m below the ground surface and 200 mm away from the flange of ISU5. Given the deep water table (11 m below ground surface) encountered at ISU5's site, PC1 was installed 4 m above the water table to avoid damage to the connection between the top of the pressure cell and the drilling rod during installation and retrieval as documented by Suleiman et al. (2010). For ISU6, shown in Figure 3(b), two push-in pressure cells (PC3 and PC4) were installed below the GWT, at approximately 10 m below the ground surface, at distances of 230 mm and 610 mm from the flange, respectively. A higher risk of damaging the PCs was deemed acceptable to measure the dissipation of pore water pressures at a deeper location, as measured by the final driven pile at ISU6. Due to space limitations, only the pore water pressure measurements are included in this paper, with complete measurements available in Ng et al. (2011a).

Pile Driving and Restrikes

Single-acting, open-ended diesel hammers were used to drive and restrike all test piles, as summarized in Table 3, and to install all reaction piles. Before driving each test pile, two 18.3 m long HP 250×62 reaction piles were driven with webs oriented parallel to adjacent piles, as shown in Figure 5. To avoid the effect of reaction pile installations on soil properties initially measured at the test pile location, the reaction piles were installed at an equal distance of 2.44 m on both sides of the test pile (see Figure 5(a)) except for ISU6 (see Figure 5(b)) where the reaction piles were installed at distances of 1.73 m and 3.12 m on either side of the test pile, since another test pile (ISU7) was included within the same test configuration but with a shallower embedded length of only 5.8 m. In all cases, the reaction piles were installed with an exposed length of 1.8 m for connection with a horizontal reaction beam. The test pile was then driven and PDA data recorded during both pile driving and restrikes. During each restrike, an average of eight hammer blows was delivered to the test pile, with the third blow selected for analyses. To help with pile setup evaluations, the time and pile embedded length before and after each restrike were precisely recorded for each test pile (see Table 3). Furthermore, pile driving resistance in terms of the total number of hammer blows per 300 mm of pile penetration (i.e.,

Manuscript Accepted Not Copyedited

hammer blow count) was accurately obtained using video. Figure 6 depicts the blow counts for ISU5, which increased from 30 at EOD to 72 at the beginning of restrike No. 6 (i.e., BOR6) over a period of 7.92-days. This substantial rise in blow count under a comparable hammer energy ratio (ETR) during driving and restrikes (with an average of 44.5% and standard deviation of 4.4%), without a significant increase in pile embedded length, is mainly caused by pile setup, ultimately increasing the pile resistance.

Dynamic Analysis Methods

With the available pile, soil, and hammer information, as well as recorded hammer blow counts, the total pile resistance for each restrike was estimated using the WEAP SPT *N*-value based method (i.e., SA method specified by Pile Dynamics, Inc., 2005). Furthermore, the PDA measured force and velocity records near the pile head were used in CAPWAP analyses to determine shaft resistance and end bearing at each event, as summarized in Table 3. Unlike WEAP, which relies on a static geotechnical analysis for an assessment of resistance distribution, CAPWAP quantifies the total static resistance as well as its distribution along the pile length and the end bearing component.

Static Load Tests

Following completion of all restrikes, vertical SLTs were performed on test piles following the "Quick Test" procedure of ASTM D1143 (2007), according to the schedule indicated in Table 3. In addition to recording the strain data along the pile shaft, four 250 mm stroke displacement transducers, installed at the four extreme edges of the test pile flanges, recorded the pile vertical movement during each loading and unloading step. For each pile, the pile resistance (or the total nominal resistance) was calculated using the measured load-displacement curve and the Davisson's (1972) criterion, while the variation in pile force along the depth was estimated using the measured strain data at every load step, as shown in Figure 7. Residual stresses were not accounted for in the load distribution, due to: 1) insignificant change in measured pile stresses on ISU5 (-0.54% to 0.82% at EOD); and 2) no effect on total pile resistance, which is the target parameter to be quantified in the companion paper. By extending the pile force resistance versus pile length strain curves to the pile toe, the end bearing contribution was also estimated. The nominal pile resistance of ISU5 was found to be 1081 kN, and its distribution along the pile length is shown in Figure 7 (by the solid line without markers) as established from interpolation

Manuscript Accepted Not Copyedited

of the force distribution curves corresponding to 1051 kN and 1114 kN. In this case, the end bearing component was 247 kN or 23% of the total pile resistance of 1081 kN. Subtracting the end bearing resistance from the total nominal pile resistance, the shaft resistance for ISU5 was determined to be 834 kN. Table 3 lists the shaft resistance and end bearing for all piles except ISU4 and ISU6, for which several strain gauges failed during the tests and thus this information could not be evaluated with sufficient accuracy.

RESULTS

Observed Pile Setup

In addition to the increase in hammer blow counts observed in Figure 6 between EOD condition and BOR6 for ISU5, Table 4 summarizes the percent of pile resistance increase at different times (ΔR_t) with reference to the calculated pile resistance at EOD (R_{EOD}) from CAPWAP analyses. The increases in total pile resistance, shaft resistance and end bearing resistance are listed separately to illustrate the different effects of setup. Both shaft resistance and end bearing increased with time after EOD. Referring to the last restrikes of all test piles, the increase in CAPWAP calculated shaft resistance ranged from 51% to 71% while the end bearing resistance increases varied between 8% and 21%. Since the end bearing component on average was about 16% of the total resistance, the impact of setup estimated for this component is not significant. The good correlation between the increase in CAPWAP's shaft resistance and the static load test result, which indicates 52% to 66% increase in shaft resistance, emphasizing that the setup largely affects the shaft resistance.

Logarithmic Trend

When plotted as a function of time (t), the percent increase in total resistance, shaft resistance and end bearing, with respect to the corresponding resistance at EOD ($\Delta R_t/R_{EOD}$ in Table 4) obtained using CAPWAP, generally followed a logarithmic trend for ISU5, as shown in Figure 8. This illustrates that total, shaft and end bearing resistances increased immediately after EOD with rapid gains within the first day, followed by an increase at a slower rate after the second day. The same observation holds for the calculated total resistance from WEAP. Note that the trend lines of WEAP and CAPWAP are different, because different R_{EOD} values were estimated (see Table 3). Furthermore, the extrapolated WEAP and CAPWAP logarithmic trends provide good estimates of the measured pile resistance from SLT.

Manuscript Accepted Not Copyedited

Pore Water Pressure

Given that PC1 at ISU5 was installed above the groundwater table and due to space limitations, only the results of ISU6 are explicitly described herein. The percent change in pore water pressures with respect to the hydrostatic pressure of 63 kPa recorded at ISU6 using PC3 and PC4 at 10 m below ground surface, with the groundwater table at 4.6 m, are plotted in Figure 9 as function of time. Figure 9(a) shows the recorded data for the first 20 minute period. Accordingly, pore water pressure recorded using PC3 experienced a slight reduction in readings before the pile toe reached the depth of the device, but no significant change was recorded as the pile passed by the gauge location during driving. The recorded pore pressure progressively increased from 34% to 61% at PC3 and from -12% to 2% at PC4 between the time when the pile passed through the devices and BOR3. After BOR3, fluctuations in data during restrike and SLT, as well as gradual dissipation of pressure with time, were generally seen (Figure 9(b)). For PC3, which was closer to the pile, the pore water pressure dissipation generally followed a logarithmic trend and reduced to 9% within a day (i.e., around BOR5), almost returning to its hydrostatic state, which indicates complete dissipation in about eight days (i.e., about one day after BOR7). Unfortunately, PC3 failed to record any measurements thereafter. The dissipated PC3 pore water pressure as a percentage of the pressure measured at EOD as a function of time (t) was best fitted with a logarithmic trend with a relatively high coefficient of determination (R^2) of 0.79 shown in Figure 10. Within one day after EOD, both the percent increase in total resistance and dissipated pore water pressure are comparable (i.e., both are about 30% at one day). The minimal difference in the gradients (i.e., 0.55 for resistance and 0.50 for pore water pressure dissipation as shown in equations included in Figure 10) suggests that the logarithmic increase in total pile resistance followed the rate of the pore water pressure dissipation. The difference between the increase of pile resistance and the percent of pore water pressure dissipation curves, which is mainly due to the difference in the intercept values of 0.33 for resistance and 0.25 for pore water pressure as shown by equations presented in Figure 10, is believed to be due to remolding and healing processes occurring in the soil disturbed by pile driving.

Influence of Soil Properties

Since the pile setup largely increases the shaft resistance, a detailed correlation study between soil properties and increase in unit shaft resistance (Δf) was performed. The increase in unit shaft resistance calculated for ISU5 using CAPWAP between EOD and the last restrike was

Manuscript Accepted Not Copyedited

plotted along the embedded pile length in Figure 11 together with the measured vertical coefficient of consolidation (C_v) and SPT *N*-value. A similar distribution of Δf for the SLT, the difference between the measured unit shaft resistance from SLT at 9 days after EOD and the CAPWAP calculated unit shaft resistance at EOD are also included in Figure 11 for comparative purposes. It is noted that the distributions of Δf for both CAPWAP and SLT have a similar trend. Referring to the Δf distribution based on SLT (dashed line), Figure 11 shows that the Δf increased by about 15 kN/m^2 in the top 5 m thick soil layer, which was characterized with relatively small S_u value of 97 kPa and SPT *N*-values ranging between 6 and 8. The Δf continued to reduce to a depth of about 11 m from the ground surface, where the surrounding cohesive soil layer has the highest S_u of 211 kPa and the highest SPT *N*-value of 22. This reduction to Δf is believed to be due to the dilation of the relatively dense soil layer causing an increase in pore water pressure, which was observed during the CPT dissipation test conducted at a depth of 11.75 m. With the reduction in S_u from 211 kPa to 126 kPa and SPT *N*-value from 22 to 13 below the 11 m depth, where the surrounding soil experiences larger lateral stresses, the Δf indicated a peak increase of about 85 kN/m^2. This observation suggests that pile setup is inversely related to SPT *N*-value and S_u (or a direct relationship with the horizontal coefficient of consolidation, as indicated by Figure 4).

Quantitative Studies between Pile Setup and Soil Properties

To further expand upon the observations presented above using data from ISU5, the percent increase in total pile resistance, shaft resistance and end bearing estimated for all five test piles using CAPWAP were compared with weighted average SPT *N*, S_u, and C_h values, allowing variation of soil layer thicknesses along the embedded pile length to be included. For soil layers where the CPT dissipation test was not conducted, or the 50% consolidation was not achieved, the horizontal coefficient of consolidation (C_h) was estimated using the SPT *N*-value based on the correlation developed from field test results, presented in Figure 4. Table 2 summarizes the findings together with the weighted average soil properties along the pile shaft and near the pile toe for each test site, while Figure 12 presents graphical representations of the same data for each of the soil variables affecting pile setup at a common time of approximately 1 day after EOD to illustrate the effect of soil properties, not time, on setup. Figure 12(a) and (b) quantify that the increase in total pile resistance and shaft resistance is inversely proportional to SPT *N*-value and S_u for all five piles while Figure 12(c) shows a linear relationship between both the total and

Manuscript Accepted Not Copyedited

shaft resistances with the C_h value. Although the end bearing components were included in these figures, no clear correlations between the soil properties and the end bearing component are evident. This is largely due to relatively significant scatter in the data resulting from: a) smaller contributions of the end bearing to the total pile resistance; and b) small errors in the estimation of shaft resistance, causing larger error to the end bearing component. The insignificant impact of the end bearing on pile setup was also confirmed by the comparable trends observed for both the shaft resistance and total pile resistance. Most importantly, Figure 12 strongly supports the conclusion that an opportunity exists for routine in-situ (i.e., SPTs and/or CPTs with pore pressure dissipation tests) to quantitatively estimate pile setup. This topic is further investigated in the companion paper (Ng et al., 2011b).

CONCLUSIONS

Motivated by insufficient information on pile setup of small-displacement piles in the literature, a detailed experimental investigation was conducted to quantify the pile setup for widely used steel H-piles. From the analyses of the pile and soil test data, the following conclusions were drawn:

1. Tested steel H-piles experienced the effects of setup along the pile shaft and at the pile toe in cohesive soils, with the setup influencing the shaft resistance more than the end bearing. With respect to the CAPWAP estimated pile resistance at EOD, the increase in the shaft resistance due to setup was between 51% and 71%, whereas the corresponding increase of the end bearing component was between 8% and 21%. The overall impact of the setup was even smaller because its average contribution to the total resistance at EOD was about 16%. The influence of pile setup was also evident by the significant increase in pile driving resistance in terms of hammer blow counts recorded between EOD and BORs. All of these observations were confirmed by the static load test measurements.
2. As expected and documented by other researchers, the gain in total pile resistance for steel H-piles exhibited a linear trend with the logarithm of time. The same trend was also true for the shaft resistance and the end bearing components. All pile resistances increased immediately and significantly within a day after EOD and continuously increased at a slower rate after the second day. A comparison of the gradients of the best fits obtained for various data revealed that the logarithmic increase in total pile resistance

Manuscript Accepted Not Copyedited

generally followed the rate of pore water pressure dissipation.

3. The experimental investigation confirmed that the amount of setup at a given time depends on soil properties, including the coefficient of consolidation, S_u, and SPT N-value. Piles embedded in a softer cohesive soil with a larger horizontal coefficient of consolidation, characterized by smaller SPT N and S_u values, exhibited higher percentage increases in total pile resistances. Correspondingly, lower setup effects were observed for piles embedded in denser soils. The collected experimental data provided sufficient information for quantifying pile setup using surrounding soil properties, which is rarely available in the published literature. Based on the field test experience, it is suggested that including CPT pore water pressure dissipation tests as part of the site investigation will not only help determine the coefficient of consolidation but also allow the change in pore water pressure that influences pile setup to be estimated.
4. The successful correlation between pile setup and certain soil properties suggest that it may be possible to establish a cost-effective means to estimate pile setup using SPT N, S_u and/or CPTs with pore water pressure dissipation tests. Detailed laboratory soil classifications and soil layer identifications are also required. This approach promises greater economy than one that requires restrike testing while lacking the knowledge of relevant soil properties.

A systematic investigation on the quantification of pile setup in terms of the surrounding soil properties is presented in the companion paper.

ACKNOWLEDGMENTS

The authors express their gratitude to Iowa Highway Research Board for sponsoring this project and members of the project's Technical Advisory Committee for their guidance and advice: Ahmad Abu-Hawash, Dean Bierwagen, Lyle Brehm, Ken Dunker, Kyle Frame, Steve Megivern, Curtis Monk, Michael Nop, Gary Novey, John Rasmussen and Bob Stanley. The authors would like to thank various bridge and soil contractors for their contributions to the field tests.

Manuscript Accepted Not Copyedited

REFERENCES

AbdelSalam, S. S., Sritharan, S., and Suleiman, M. T. (2010). "Current Design and Construction Practices of Bridge Pile Foundations with Emphasis on Implementation of LRFD." *Journal of Bridge Engineering*, ASCE, 15(6), 749-758. (http://cedb.asce.org/cgi/WWWdisplay.cgi?271422)

American Association of State Highway and Transportation Officials (AASHTO). (2010). *LRFD Bridge Design Specifications Customary U.S. Units 5th Edition*, Washington, D.C.

American Standard Test Method (ASTM) Standard D2435. (2004). *Standard Test Methods for One-Dimensional Consolidation Properties of Soils Using Incremental Loading*, ASTM International, West Conshohocken, PA.

American Standard Test Method (ASTM) Standard D1143. (2007). *Standard Test Methods for Deep Foundations Under Static Axial Compressive Load*, ASTM International, West Conshohocken, PA.

Casagrande, A. (1936). "Determination of the Preconsolidation Load and its Practical Significance." *Proceedings of 1st International Conference on Soil Mechanics and Foundation Engineering*, Cambridge, MA, Vol. 3, 60-64.

Davisson, M. (1972). "High Capacity Piles". *Proceedings, Soil Mechanics Lecture Series on Innovations in Foundation Construction*, ASCE, IL Section, Chicago, IL, 81–112.

Fellenius, B. H. (2002). "Pile Dynamics in Geotechnical Practice - Six Case Histories." *Geotechnical Special Publication No. 116*, ASCE, Proceedings of International Deep Foundations Congress 2002, Feb 14-16, M. W. O'Neill and F. C. Townsend, ed., Orlando, FL, 619-631.

Houlsby, G., & Teh, C. (1988). "Analysis of the Piezocone in Clay." *Penetration Testing 1988*, 2, 777-783.

Huang, S. (1988). "Application of Dynamic Measurement on Long H-Pile Driven into Soft Ground in Shanghai." *Proceedings of 3rd International Conference on the Application of Stress-Wave Theory to Piles*, B. H. Fellenius, ed., Ottawa, Ontario, Canada, 635-643.

Manuscript Accepted Not Copyedited

Journal of Geotechnical and Geoenvironmental Engineering, 139(2), February 2013, pp. 199-209

Komurka, V. E., Wagner, A. B., and Edil, T. B. (2003). "Estimating Soil/Pile Set-Up." *Final Report*. Wagner Komurka Geotechnical Group, Inc. and University of Wisconsin-Madison, WI.

Long, J. H., Kerrigan, J. A., and Wysockey, M. H. (1999). "Measured Time Effects for Axial Capacity of Driving Piling." *Transportation Research Record 1663*, Paper No. 99-1183, Transportation Research Board, Washington, D.C., 8-15.

Long, J. H., Maniaci, M., and Samara, E. A. (2002). "Measured and Predicted Capacity of H-Piles." *Geotechnical Special Publication No.116,* Advances in Analysis, Modeling & Design, Proceedings of International Deep Foundations Congress 2002, ASCE, Feb 14-16, M. W. O'Neill and F. C. Townsend, ed., Orlando, FL, 542-558.

Lukas, R. G., and Bushell, T. D. (1989). "Contribution of Soil Freeze to Pile Capacity." Foundation Engineering: Current Principles and Practices, Vol. 2. Fred H. Kulhawy, ed., ASCE, 991-1001.

Mayne, P. W. (2001). "Stress-Strain-Strength-Flow Parameters from Enhanced In-Situ Tests." *Proceedings of International Conference on In-Situ Measurement of Soil Properties and Case Histories*, Bali, Indonesia, 27-48.

Ng, K. W. (2011). "Pile Setup, Dynamic Construction Control, and Load and Resistance Factor Design of Vertically-Loaded Steel H-Piles." *Ph. D. Dissertation*. Department of Civil, Construction, and Environmental Engineering, Iowa State University, Ames, IA.

Ng, K. W., Suleiman, M. T., Sritharan, S., Roling, M., and AbdelSalam, S. S. (2011a). "Development of LRFD Design Procedures for Bridge Pile Foundations in Iowa – Field Testing of Steel Piles in Clay, Sand and Mixed Soils and Data Analysis." Final Report Vol. II. IHRB Project No. TR-583. *Institute for Transportation*, Iowa State Univeristy, Ames, IA. (http://srg.cce.iastate.edu/lrfd/)

Ng, K.W., Suleiman, M.T., and Sritharan, S. (2011b). "Pile Setup in Cohesive Soil: Analytical Quantifications and Design Recommendations." *Journal of Geotechnical and Geoenvironmental Engineering*, ASCE (Under Review).

Manuscript Accepted Not Copyedited

Journal of Geotechnical and Geoenvironmental Engineering, 139(2), February 2013, pp. 199-209

Pei, J., and Wang, Y. (1986). "Practical Experiences on Pile Dynamic Measurement in Shanghai." *Proceedings of International Conference on Deep Foundations*, Beijing, China, 2.36-2.41.

Pile Dynamics, Inc. (2005). *GRLWEAP Wave Equation Analysis of Pile Driving: Procedures and Models Version 2005*. Cleveland, OH.

Randolph, M. F., Carter, J. P., and Wroth, C. P. (1979). "Driven Piles in Clay - The Effects of Installation and Subsequent Consolidation." *Geotechnique*, 29(4), 361-393.

Robertson, P. K., Campanella, R. G., and Wightman, A. (1983). "SPT–CPT Correlations." *Journal of the Geotechnical Engineering Division*, Vol. 108, No. GT 11, 1449-1459.

Skov, R., and Denver, H. (1988). "Time-Dependence of Bearing Capacity of Piles." *Proceedings of 3rd International Conference on the Application of Stress-Wave Theory to Piles*, B. H. Fellenius, ed., Ottawa, Ontario, Canada, pp.879–888.

Soderberg, L. O. (1962). "Consolidation Theory Applied to Foundation Pile Time Effects." *Geotechnique*, 12(3), 217-225.

Suleiman, M. T., Stevens, L., Jahren, C. T., Ceylan, H., and Conway, W. M. (2010). "Identification of Practices, Design, Construction, and Repair Using Trenchless Technology". *Institute for Transportation*, Final Research Report. Iowa Department of Transportation Project Number IHRB-06-09.

Svinkin, M. R., and Skov, R. (2000). "Set-Up Effect of Cohesive Soils in Pile Capacity." *Proceedings of 6th International Conference on the Application of Stress-Wave Theory to Piles*, Edited by Niyama, S., and Beim, J., Sao Paulo, Brazil, pp.107–111.

Manuscript Accepted Not Copyedited

Journal of Geotechnical and Geoenvironmental Engineering, 139(2), February 2013, pp. 199-209

Table 1. Summary of soil profiles and results of soil tests for all test sites

Test pile	Soil depth (m)	USCS soil classification	Ave. SPT *N*-value at each layer	Unit weight (kN/m^3)	*LL* (%)	*PI* (%)	*OCR*[a] (sample depth in m)	C_v (cm^2/min)	C_h[b] (cm^2/min); Depth in m	C_h[d] (cm^2/min)
ISU2	0 to 4.88	Clayey sand (SC)	3	-	28.7	13.4	1.0 (2.7)	0.152	-	-
	4.88 to 6.1	Low plasticity clay (CL)	14	19.1	43.7	25.0	1.1 (6.1)	0.052	-	-
	6.1 to 10.98	Low plasticity clay (CL)	3	22.3	43.2	19.2	1.1 (9.1)	0.126	0.892; 10.8	1.246
	10.98 to 13.42	Clay	4	-	-	-	-	-	-	-
	13.42 to 17.03	Low plasticity clay (CL)	4	23.0	47.5	28.4	1.0 (16.8)	0.113	-	-
ISU3	0 to 2.35	Sandy low plasticity clay (CL)	-	-	36.5	18.7	4.7[c] (0.9)	0.072	-	-
	2.35 to 10.37	Sandy low plasticity clay (CL)	8	19.1	21.4	4.5	1.5 (8.2)	0.077	0.192; 6.8	0.168
	10.37 to 15.55	Low plasticity clay w/ sand (CL)	10	19.0	30.6	10.8	1.3 (15.2)	0.041	-	-
ISU4	0 to 2.35	Sandy low plasticity clay (CL)	3	19.7	29.3	11.4	-	-	-	-
	2.35 to 2.7	Well graded sand w/ clay (SW-SC)	-	21.2	-	-	-	-	-	-
	2.7 to 6.05	Silty sand (SM)	5	20.2	-	-	-	-	-	-
	6.05 to 6.45	Well graded sand (SW)	-	21.6	-	-	-	-	-	-
	6.45 to 12.55	Low plasticity clay w/ sand (CL)	12	22.2	27.5	13.5	1.6 (8.2)	0.077	0.036; 6.4 0.019; 6.5	0.133 0.099
	12.55 to 17.31	Sandy low plasticity clay (CL)	13	21.6	26.0	13.2	1.0 (13.7)	0.076	0.009; 12.5 0.025; 15.4	0.026 0.076
ISU5	0 to 7.7	Low plasticity clay (CL)	8	20.5	38.4	20.8	4.5[c] (2.4)	0.107	-	-
							1.3 (7.6)	0.089	-	-
	7.7 to 17.5	Low plasticity clay w/ sand (CL)	16	20.3	38.6	22.2	n/a (10.7)	0.051	-	-
ISU6	0 to 4.0	Mixed fill (SC/CL)	12	-	24.8	17.2	1.2 (3.7)	0.033	-	-
	4.0 to 6.1	Silty sand (SM)	23	19.7	18.2	4.0	-	-	-	-
	6.1 to 9.0	Sandy low plasticity clay (CL)	8	19.2	24.8	10.9	-	-	-	-
	9.0 to 9.3	Sandy to silty sand seam	10	-	-	-	-	-	-	-
	9.3 to 15.5	Sandy low plasticity clay (CL)	21	23.5	26.7	13.1	1.1 (14.9)	0.039	0.008; 15.2	0.058
	15.5 to 19.05	Silt (ML)	22	20.6	31.0	23.6	n/a (18)	0.057	-	-

[a] Estimated using Casagrande (1936) graphical procedure from one-dimensional consolidation test.
[b] Estimated from CPT with pore pressure dissipation test using strain path method, and rigidity index (I_R) was estimated using Mayne's (2001) method.
[c] Unusual high OCR due to mechanical compaction during road construction.
[d] Estimated from CPT using strain path method, and rigidity index (I_R) was estimated as the ratio of shear modulus (G) to undrained shear strength (S_u).

Manuscript Accepted Not Copyedited

Table 2. Weighted average soil properties along pile shaft and near pile toe

Test pile	SPT *N*-value		S_u (kPa)		C_h (cm^2/min)	
	Shaft	Toe	Shaft	Toe	Shaft	Toe
ISU2	5	4	83	56	0.208	0.178
ISU3	8	10	124	152	0.045	0.026
ISU4	10	13	133	123	0.056	0.015
ISU5	12	13	116	126	0.028	0.015
ISU6	14	22	140	275	0.022	0.005

Manuscript Accepted Not Copyedited

Table 3. Summary of the five test piles and their results

Test pile	Hammer	Type of event	Time after EOD, *t* (min, hr or day)	Embedded pile length (m)	Blows per 300 mm	WEAP total resistance (kN)	CAPWAP pile resistance (kN)			SLT pile resistance (kN)			
							Total	Shaft	End Bearing	Total[c]	Shaft	End Bearing	Peak[d]
ISU2	Delmag D19-42	EOD	0	16.46	10	343	359	297	63				
		BOR1	4.08[b]	16.77	14	448	517	451	66	556	492	64	573
		BOR2	22.08[b]	16.87	18	547	578	508	70		(9 days after EOD)		
		BOR3	2.97	17.02	22	617	578	507	71				
ISU3	Delmag D19-32	EOD	0	14.63	10	363	439	379	60				
		BOR1	4.10[a]	14.79	16	493	459	393	66				
		BOR2	10.51[a]	14.94	16	493	467	398	69	667	605	62	667
		BOR3	16.7[a]	15.09	16	493	577	504	73		(36 days after EOD)		
		BOR4	1.11	15.30	18	539	637	564	73				
		BOR5	1.96	15.55	20	586	657	584	73				
ISU4	Delmag D19-42	EOD	0	16.77	13	422	453	392	60				
		BOR1	5.83[a]	16.87	15	472	469	398	71				
		BOR2	22.75[a]	16.97	18	543	484	414	71	685	Incomplete Readings		694
		BOR3	57.60[a]	17.09	16	497	538	476	62		(16 days after EOD)		
		BOR4	17.76[b]	17.18	21	592	601	532	69				
		BOR5	1.74	17.25	24	653	642	573	69				
		BOR6	4.75	17.31	26	687	685	616	69				
ISU5	Delmag D16-32	EOD	0	16.77	30	636	790	550	240				
		BOR1	7.75[a]	16.87	36	791	842	600	243				
		BOR2	18.14[a]	16.97	37	809	957	713	244	1081	834	247	1170
		BOR3	1.15[b]	17.07	38	823	979	732	246		(9 days after EOD)		
		BOR4	22.08[b]	17.15	44	902	1035	778	257				
		BOR5	2.90	17.22	54	1013	1044	787	258				
		BOR6	7.92	17.28	72	1140	1088	829	259				
ISU6	Delmag D19-42	EOD	0	16.87	21	615	644	546	98				
		BOR1	2.30[a]	16.96	20	590	644	547	97				
		BOR2	6.28[a]	17.04	22	632	662	558	104				
		BOR3	16.85[a]	17.12	25	679	658	553	105	946	Incomplete Readings		946
		BOR4	1.61[b]	17.18	29	739	786	678	109		(14 days after EOD)		
		BOR5	19.92[b]	17.27	38	879	831	721	110				
		BOR6	2.82	17.35	44	965	875	762	113				
		BOR7	6.79	17.41	53	1065	938	823	115				
		BOR8	9.81	17.44	60	1121	937	823	114				

[a] Time in minutes; [b] Time in hours; [c] Pile resistance based on Davisson's criterion; and [d] Maximum sustainable test load measured during SLT.

Manuscript Accepted Not Copyedited

Table 4. Percentage increase in pile resistance based on WEAP, CAPWAP and SLT

Test pile	Type of event	Time after EOD, *t* (minute, hour or day)	WEAP, $\Delta R_t/R_{EOD}$ (%)	CAPWAP, $\Delta R_t/R_{EOD}$ (%)			SLT			
							$\Delta R_t/R_{EOD\text{-}WEAP}$ (%)	$\Delta R_t/R_{EOD\text{-}CAPWAP}$ (%)		
				Total	Shaft	End Bearing	Total	Total	Shaft	End Bearing
ISU2	BOR1	4.08[b]	31 %	44 %	52 %	6 %	62 %	55 % (9 days after EOD)	66 %	3 %
	BOR2	22.08[b]	59 %	61 %	71 %	12 %				
	BOR3	2.97	80 %	61 %	71 %	13 %				
ISU3	BOR1	4.10[a]	36 %	4 %	4 %	10 %	84 %	52 % (36 days after EOD)	60 %	3 %
	BOR2	10.51[a]	36 %	6 %	5 %	16 %				
	BOR3	16.7[a]	36 %	31 %	33 %	22 %				
	BOR4	1.11	49 %	45 %	49 %	21 %				
	BOR5	1.96	61 %	49 %	54 %	21 %				
ISU4	BOR1	5.83[a]	12 %	4 %	1 %	17 %	62 %	51 % (16 days after EOD)	Incomplete Readings	
	BOR2	22.75[a]	29 %	7 %	5 %	17 %				
	BOR3	57.60[a]	18 %	19 %	19 %	15 %				
	BOR4	17.76[b]	40 %	33 %	36 %	14 %				
	BOR5	1.74	55 %	42 %	46 %	13 %				
	BOR6	4.75	63 %	51 %	57 %	14 %				
ISU5	BOR1	7.75[a]	24 %	7 %	9 %	1 %	70 %	37 % (9 days after EOD)	52 %	3 %
	BOR2	18.14[a]	27 %	21 %	30 %	2 %				
	BOR3	1.15[b]	30 %	24 %	33 %	3 %				
	BOR4	22.08[b]	42 %	31 %	41 %	7 %				
	BOR5	2.90	59 %	32 %	43 %	7 %				
	BOR6	7.92	79 %	38 %	51 %	8 %				
ISU6	BOR1	2.30[a]	-4 %	0 %	0 %	0 %	54 %	47 % (14 days after EOD)	Incomplete Readings	
	BOR2	6.28[a]	3 %	3 %	2 %	6 %				
	BOR3	16.85[a]	10 %	2 %	1 %	7 %				
	BOR4	1.61[b]	20 %	22 %	24 %	11 %				
	BOR5	19.92[b]	43 %	29 %	32 %	12 %				
	BOR6	2.82	57 %	36 %	40 %	15 %				
	BOR7	6.79	73 %	46 %	51 %	17 %				
	BOR8	9.81	82 %	46 %	51 %	16 %				

[a] Time in minutes.
[b] Time in hours.

Manuscript Accepted Not Copyedited

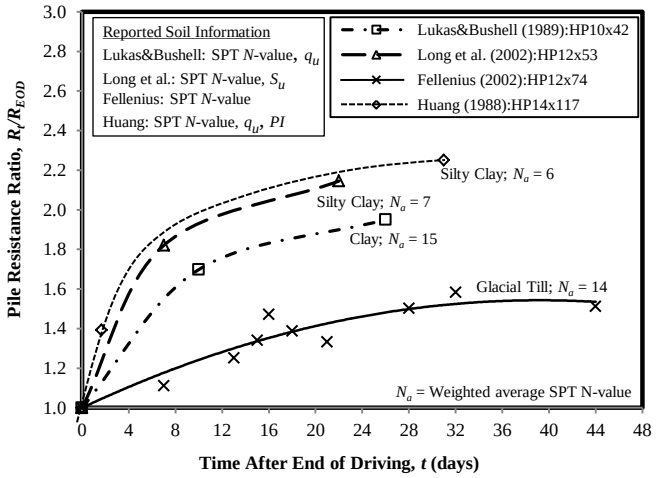

Figure 1. Summary of steel H-pile resistance ratios from literature

Manuscript Accepted Not Copyedited

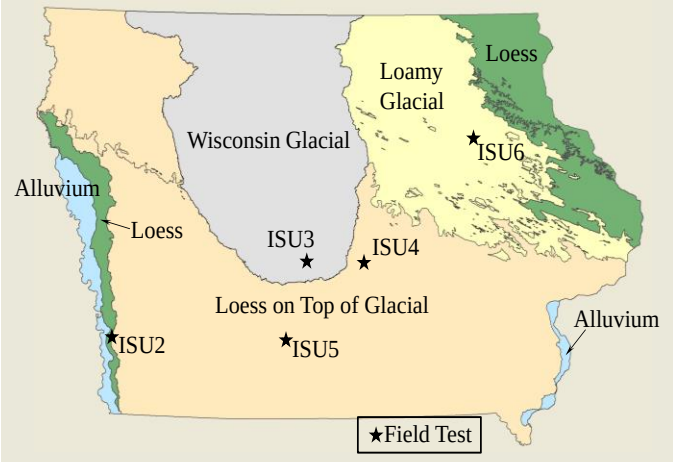

Figure 2. Locations of steel H-piles tested in the state of Iowa

Manuscript Accepted Not Copyedited

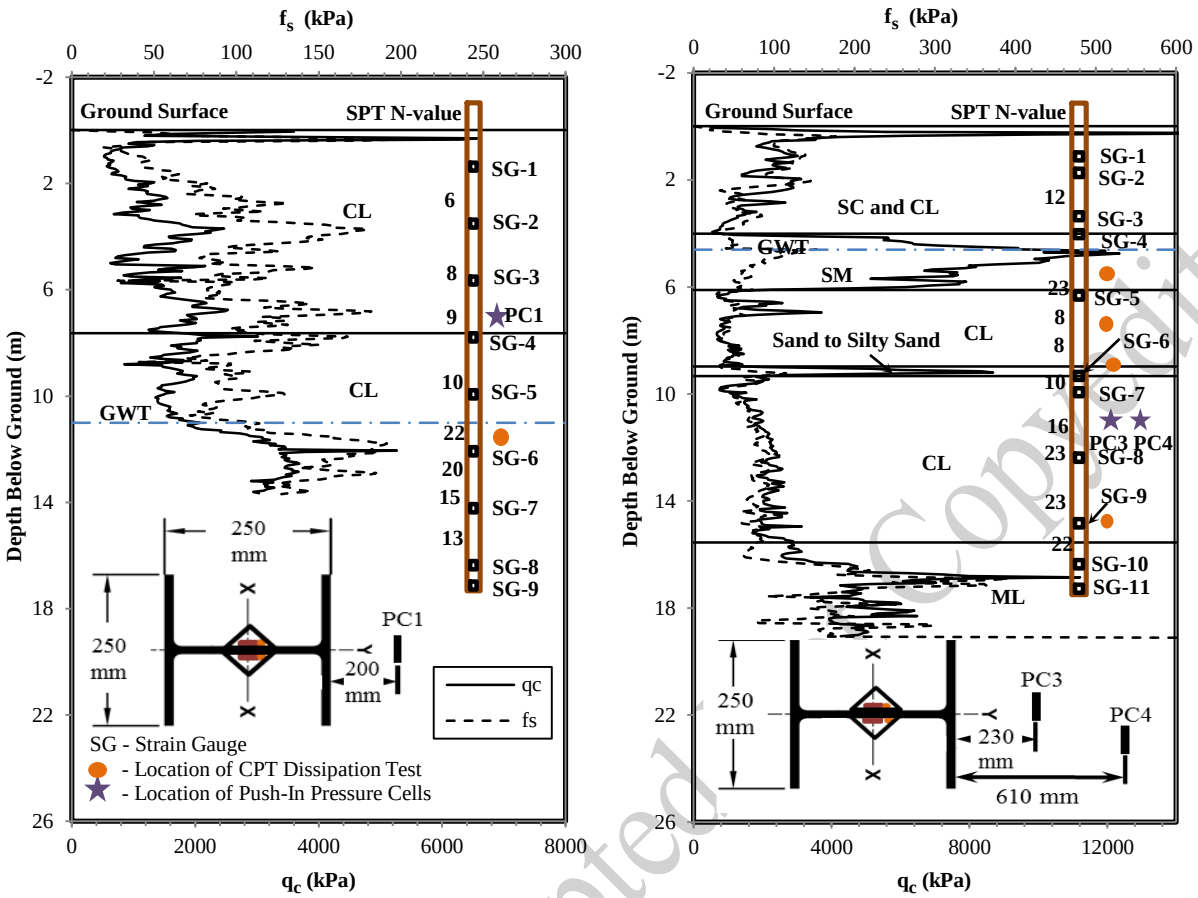

(a) For ISU5 (b) For ISU6

Figure 3. Soil profiles, soil test results and test pile instrumentation schematics

Manuscript Accepted. Copyrighted

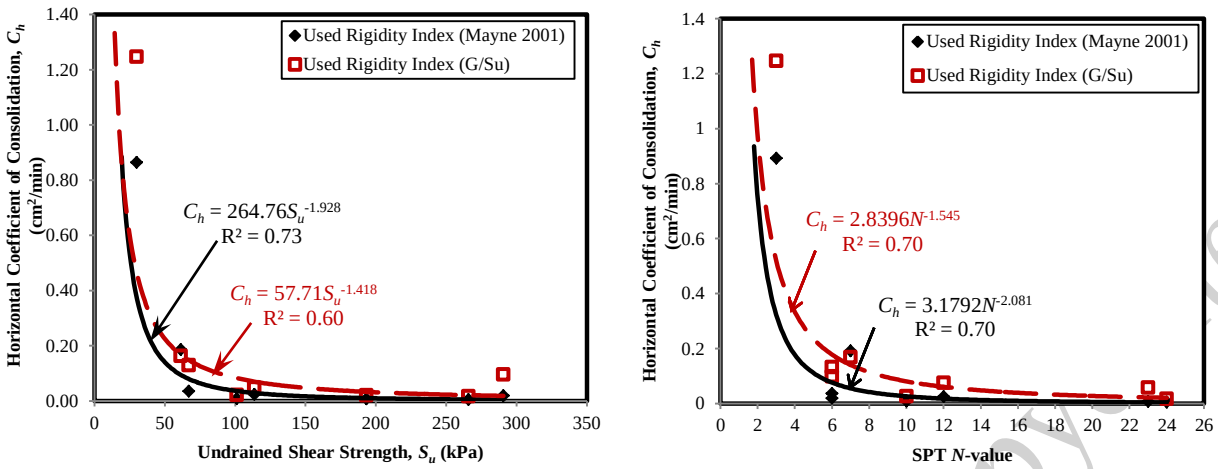

(a) C_h versus undrained shear strength (S_u) (b) C_h versus SPT N-value

Figure 4. Proposed relationships between horizontal coefficient of consolidation and: (a) undrained shear strength (S_u); (b) SPT N-value

Manuscript Accepted Not Copyedited

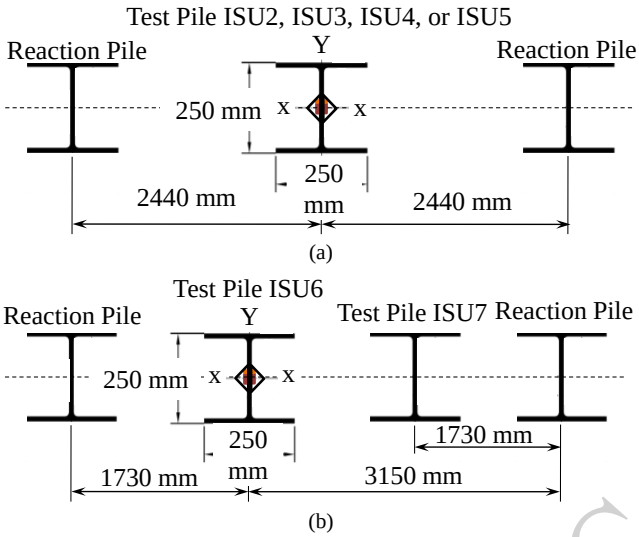

Figure 5. Plan view of test configuration for reaction piles and test pile for (a) ISU2, ISU3, ISU4, and ISU5; and (b) ISU6 and ISU7

Manuscript Accepted Not Copyedited

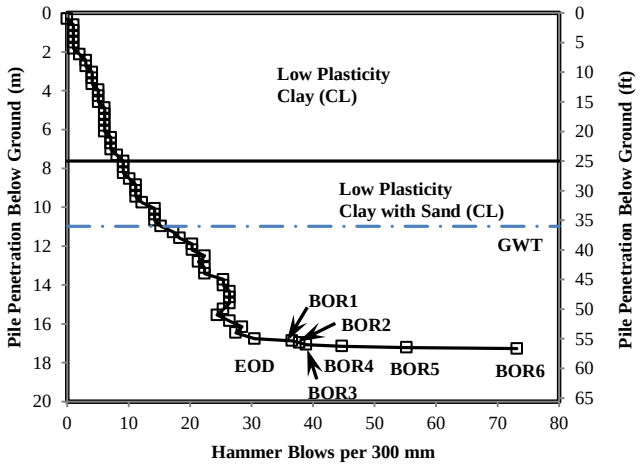

Figure 6. Pile driving resistance observed for ISU5

Manuscript Accepted Not Copyedited

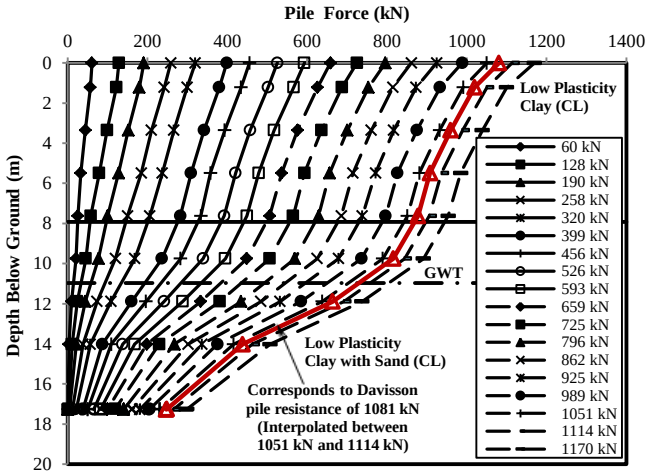

Figure 7. Measured force distribution along the pile length during SLT at each load increment for ISU5

Manuscript Accepted Not Copyedited

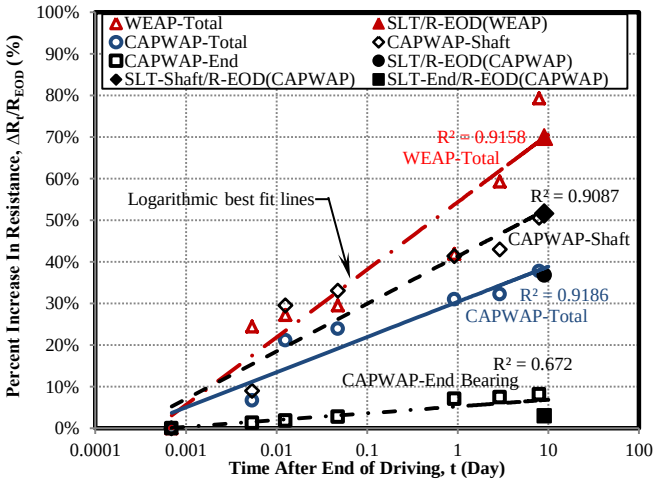

Figure 8. Estimated and measured percent increase in pile resistance for ISU5 with time after EOD in a logarithmic scale

Manuscript Accepted Not Copyedited

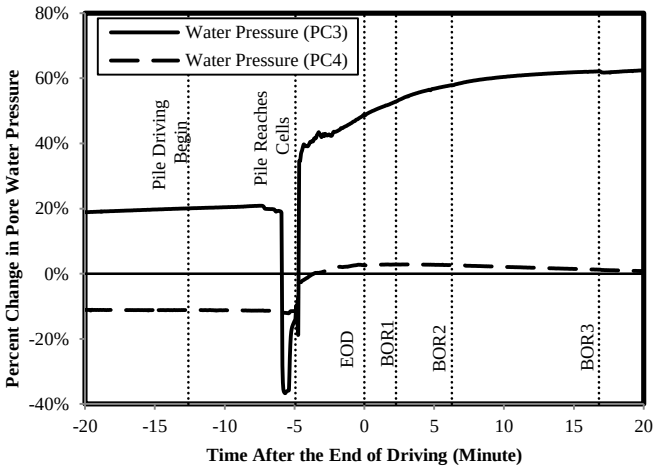

(a) Time in minutes

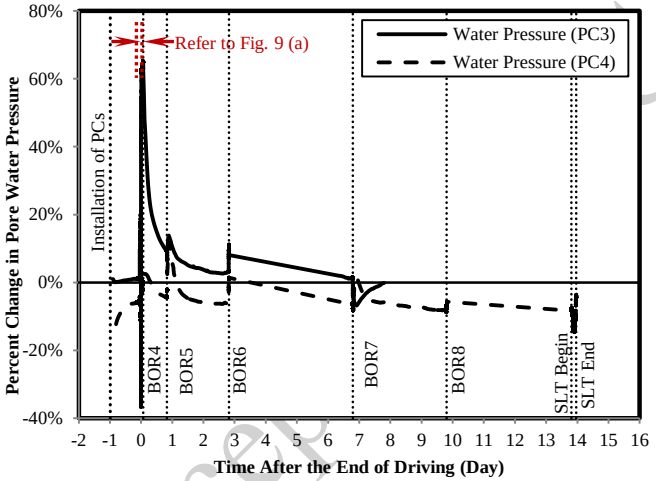

(b) Time in days

Figure 9. Percent change in pore water pressure recorded by push-in pressure cells (PC3 and PC4) at ISU6 as function of time considered after EOD in (a) minutes; and (b) days

Manuscript Accepted Copyedited

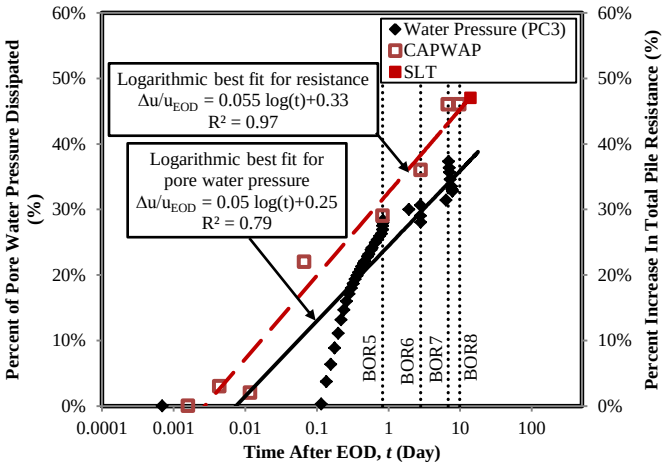

Figure 10. Comparison between pore water pressure dissipation and pile setup for ISU6

Manuscript Accepted Not Copyedited

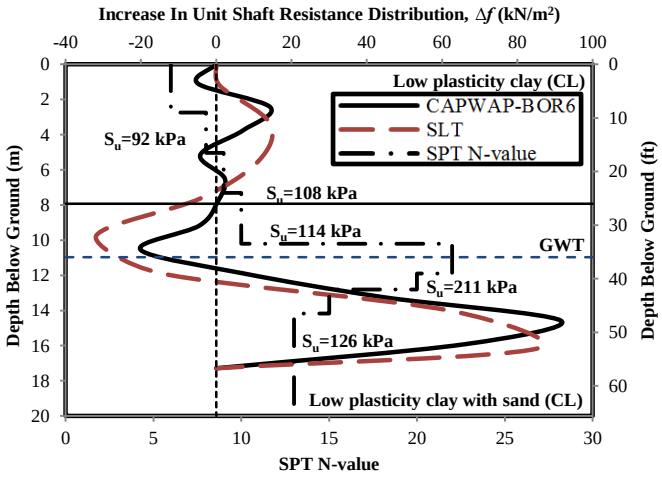

Figure 11. Relationship between increase in unit shaft resistance and soil properties for ISU5

Manuscript Accepted Not Copyedited

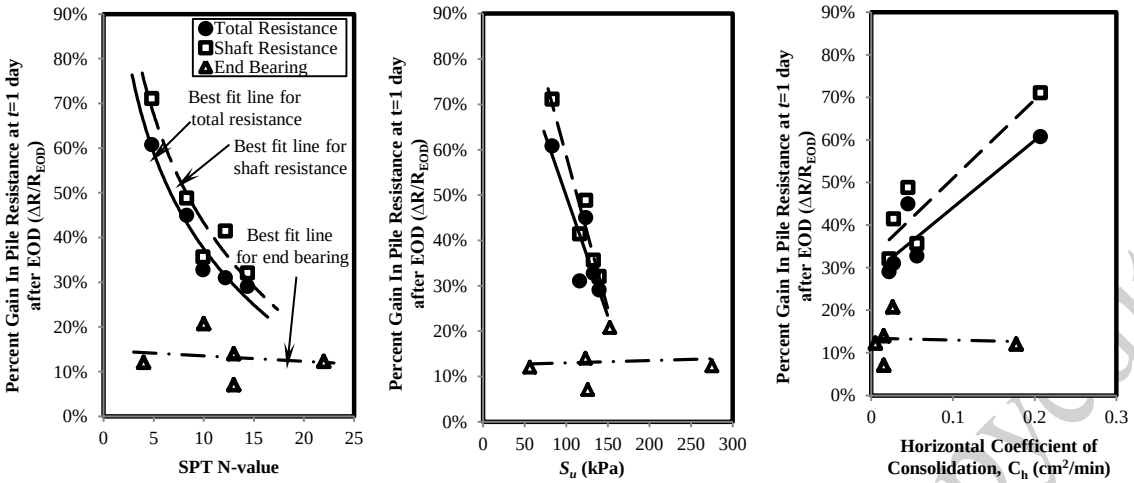

(a) Relationship with SPT *N*-value (b) Relationship with *Su* (c) Relationship with C_h

Figure 12. Relationships between percent gain in pile resistances estimated at a time of 1 day after EOD for all sites and (a) SPT *N*-value, (b) S_u, and (c) C_h

Manuscript Accepted Not Copyedited

Figure Caption List

Figure 1. Summary of steel H-pile resistance ratios from literature

Figure 2. Locations of steel H-piles tested in the state of Iowa

Figure 3. Soil profiles, soil test results and test pile instrumentation schematics

Figure 4. Proposed relationships between horizontal coefficient of consolidation and: (a) undrained shear strength (S_u); (b) SPT N-value

Figure 5. Plan view of test configuration for reaction piles and test pile for (a) ISU2, ISU3, ISU4, and ISU5; and (b) ISU6 and ISU7

Figure 6. Pile driving resistance observed for ISU5

Figure 7. Measured force distribution along the pile length during SLT at each load increment for ISU5

Figure 8. Estimated and measured percent increase in pile resistance for ISU5 with time after EOD in a logarithmic scale

Figure 9. Percent change in pore water pressure recorded by push-in pressure cells (PC3 and PC4) at ISU6 as function of time considered after EOD in (a) minutes; and (b) days

Figure 10. Comparison between pore water pressure dissipation and pile setup for ISU6

Figure 11. Relationship between increase in unit shaft resistance and soil properties for ISU5

Figure 12. Relationships between percent gain in pile resistances estimated at a time of 1 day after EOD for all sites and (a) SPT N-value, (b) S_u, and (c) C_h

Manuscript Accepted Not Copyedited

View publication stats